

Piezoelectric friction dampers for earthquake mitigation of buildings: design, fabrication, and characterization

Genda Chen[†], Gabriel T. Garrett[‡], Chaoqiang Chen^{‡†} and Franklin Y. Cheng^{‡‡}

*Department of Civil, Architectural, and Environmental Engineering, University of Missouri-Rolla,
328 Butler-Carlton Hall, 1870 Miner Circle, Rolla, MO 65409-0030, USA*

(Received August 29, 2002, Accepted August 8, 2003)

Abstract. In this paper, the design, fabrication and characterization of a piezoelectric friction damper are presented. It was sized with the proposed practical procedure to minimize the story drift and floor acceleration of an existing 1/4-scale, three-story frame structure under both near-fault and far-field earthquakes. The design operation friction force in kip was numerically determined to range from 2.2 to 3.3 times the value of the peak ground acceleration in g (gravitational acceleration). Experimental results indicated that the load-displacement loop of the damper is nearly rectangular in shape and independent of the excitation frequency. The coefficient of friction of the damper is approximately 0.85 when the clamping force on the damper is above 400 lbs. It was found that the friction force variation of the damper generated by piezoelectric actuators with 1000 Volts is approximately 90% of the expected value. The properties of the damper are insensitive to its ambient temperature and remain almost the same after being tested for more than 12,000 cycles.

Key words: piezoelectric actuators; friction damper; semi-active control; adaptive clamping force; variable friction damper; durability; seismic performance.

1. Introduction

Piezoelectric materials have dual sensing and actuating capability. They have received wide applications in aerospace engineering. However, integration of such materials into civil infrastructure systems is just beginning. The main challenge in this application is that civil engineering structures are often subjected to significantly larger strains than piezoelectric materials can endure (Housner *et al.* 1997). To meet the large strain requirement, the authors recently proposed the novel concept of piezoelectric friction damper (PFD) to control building structures (Chen and Chen 2000). As a key component of the PFD, piezoelectric stack actuators are oriented perpendicular to the sliding surfaces of the friction damper. The sliding feature of the damper makes it possible to accommodate substantial structural movement while the clamping effect on actuators limits the amount of their strains to the minimum.

[†] Associate Professor

[‡] Master Student

^{‡†} Ph.D. Student

^{‡‡} Curators' Professor Emeritus

The proposed PFD can be operated in a passive, semi-active or active state (Chen and Chen 2002a, 2002b). However, semi-active control appears to combine the best features of both passive and active systems. It requires a small amount of external power and will not cause instability through energy injection into the controlled structure. The clamping force of a semi-active friction damper can be altered based on the response of a structure being controlled. In the PFD, this is accomplished by the use of piezoelectric actuators. Due to the clamping effect, piezoelectric actuators can generate a significant amount of stress/strain when exposed to an electric field. Unlike hydraulic actuators used in variable friction dampers (Kannan *et al.* 1995), piezoelectric actuators allow for instantaneous modulation of the clamping force.

Piezoelectricity is the ability of certain crystalline materials to develop an electric charge proportional to an applied mechanical stress and a mechanical stress or strain proportional to an applied electric field. The former is referred to as the direct effect (sensing capability) and the latter, the converse effect (actuating capability). The converse effect is considered in this study. In the axial direction or “three” of a stack actuator, the constitutive equation of linear piezoelectricity describing the converse effect is expressed by (Meltzler *et al.* 1988)

$$S_3 = s_{33}^E \cdot T_3 + d_{33} \cdot E_3 \quad (1)$$

in which S_3 and T_3 represent the mechanical strain and stress, respectively, E_3 denotes the electric field applied in the axial direction, d_{33} is the piezoelectric constant which represents the electromechanical coupling of the material, and s_{33}^E means the mechanical compliance of the material measured at zero electric field or the reciprocal of the modulus of elasticity.

Significant progress has been made since the late 80's in the development of passive friction devices. A comprehensive review on this subject has been included in Chapter 4 of the book by Soong and Dargush (1997). Passive friction devices are simple in principle and have been applied into building designs. They have been shown through numerical simulations and laboratory experiments very effective for a given load. To enhance their performance in reducing the response of buildings under earthquakes of varying intensities, variable friction dampers (Kannan *et al.* 1995, Hirai *et al.* 1996) were designed and tested recently. To operate such devices, a control scheme through which a friction force is modulated must be developed. Akbay and Aktan (1990) proposed a control scheme that actively adjusts the slip force to allow slippage in controlled amounts during the response of the structure. Dowdell and Cherry (1994) proposed an “On-Off” control system where the slip force can take two values and also a system where the friction force is directly proportional to the structure's displacement state. Kannan *et al.* (1995) have proposed a “Bang-Bang” control system that changes the slip force at predetermined increments and at a fixed rate such that the slip force increases if the device slips in the previous interval, but is lowered otherwise. When the slip value reaches a predetermined limit, the clamping force is increased to its maximum. Inaudi (1997) developed a control algorithm such that the friction force is scaled to prior-local-peak value of the deformation in the damper. The clamping force remains proportional to this prior-local-peak value until another occurs in the deformation cycle. Chen and Chen (2002b) proposed a control algorithm featuring the combination of a viscous damper and a nonlinear Reid's damper.

The purpose of this study is to experimentally investigate the use of piezoelectric actuators as a means by which to vary the clamping force in a semi-active friction damper. To this endeavor, a prototype PFD is designed, fabricated, and characterized for peak response reduction and energy

dissipation of an existing $\frac{1}{4}$ scale three-story frame structure. The damper is characterized in both passive and semi-active states. The long-term durability of the damper is studied. For practical applications, a simple procedure using commercially available computer software is proposed for the design of general semi-active friction dampers (Kannan *et al.* 1995, Inaudi 1997).

2. The prototype PFD and the 3-story building structure

The piezoelectric stack actuators used in the prototype PFD were manufactured by Kinetic Ceramics, Inc (KCI). They used the PZT-100 material doped with Tungsten or PZWT-100. The piezoelectric constant, d_{33} , and the modulus of elasticity, Y_{33}^E , of the material along the axial direction or “three” are equal to 14.6×10^{-9} in/V and 6,700 ksi, respectively (O’Neil *et al.* 2000). The maximum electric field that can be applied on the actuators before depolarizing is 50 V/mil. Each stack is one inch in diameter and approximately half an inch tall. It is composed of 24 individual piezoelectric layers stack in series and wired in parallel, each 0.02 in. thick. The manufacturer provided the free displacement test results of each actuator as seen typically in Fig. 1. At a voltage of 1000 V, the free displacement is 6×10^{-4} in.

The prototype PFD is shown in Fig. 2(a) and its schematic representation is presented in Fig. 2(b). It includes four individual components based on their function. They are four preloading units, four piezoelectric stack actuators, a frictional surface sliding plate, and a steel box housing other components as indicated on Fig. 2(b). The frictional surface component is composed of a thin sheet of steel with friction material (brake linings) bonded to its top and bottom surfaces. The friction plate assembly slides against the bottom plate of the housing at its bottom surface. The top surface slides against an isolation plate that is restrained from movement in the longitudinal and lateral directions but free to move in the vertical direction. The four piezoelectric stacks are located directly above the isolation plate, each connected in series with a load cell cap and a load cell. Located above the load cell, each preloading unit consists of a preloading platform, preloading anchor, and

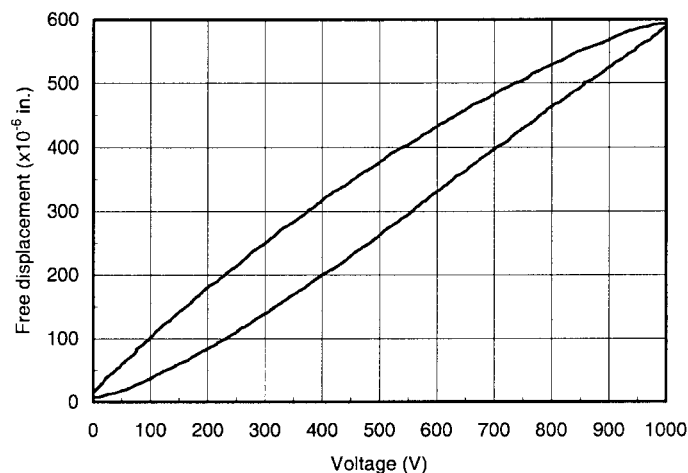
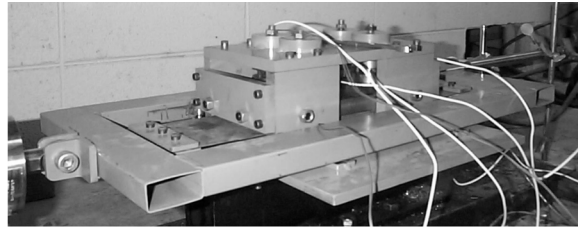
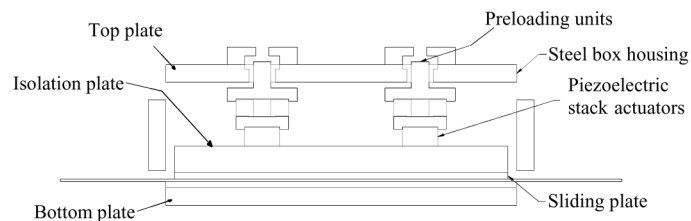


Fig. 1 Free displacement of a PZWT100 stack actuator

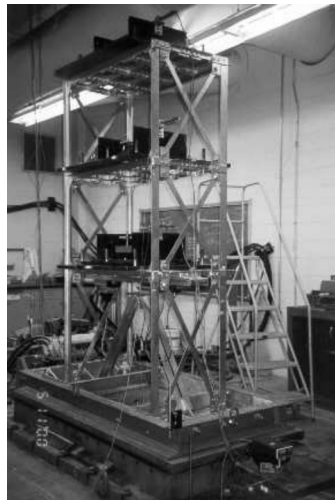


(a) Overview

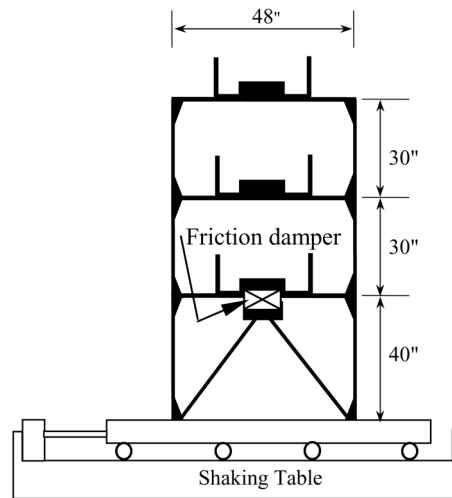


(b) Schematics

Fig. 2 The prototype PFD



(a) Overview



(b) Schematics

Fig. 3 The 3-story steel frame structure

preloading bolt. The preloading platform transfers the load from the preloading bolt to the stack. The bolt runs through a threaded hole in the preloading anchor and the preloading anchor transfers the load to the damper housing. The housing resists the internal reactions imposed by the friction surfaces and piezoelectric actuators. After the PFD was fabricated, it was found out that the basic functions of the main components of the PFD are parallel to the component functions used in the variable friction damper system by Hirai *et al.* (1996).

The 1/4-scale, 3-story building structure, shown in Fig. 3(a), is located in the highbay structures laboratory at the University of Missouri-Rolla (Tian 1997). It is 48 in. long, 24 in. wide, and 100 in. tall as schematically shown in Fig. 3(b). The natural frequencies of the structure identified from experiments are 2.62, 9.01, and 17.46 Hz and their corresponding damping ratios are 0.364%, 0.354%, and 0.267%, respectively. A computer model was established to facilitate the design of the prototype PFD. In the model, the mass of the building was lumped at three floors: 3.389 lbs·sec²/in. on the first floor, 3.368 lbs·sec²/in. on the second floor, and 3.290 lbs·sec²/in. on the third floor (top). To well calibrate the model with the measured results from shake table tests, the rigidity of each member of the building structure is explicitly simulated in the computer model by specifying various member sizes. It was observed that the model structure does not behave like a shear type of building (Tian 1997). On the shake table, a K-brace was built to facilitate the installation of the prototype PFD between the brace and the first floor.

3. Design of a PFD

3.1 A practical procedure

Two important parameters on the design of semi-active friction dampers are the range of operation friction force and the coefficient of friction. The latter can be determined based on laboratory tests on the friction materials chosen. The optimum friction force for building structure applications depends on the performance index, structural properties and characteristics of external disturbance. The previous study by Chen and Chen (2002c) has demonstrated that, under harmonic loading, a Coulomb friction damper could be as effective as a semi-active friction device even though the latter is generally more effective than the former in reducing earthquake-induced responses. Therefore, it is recommended that, for simplicity in practical applications, a PFD be designed based on the performance of a Coulomb friction damper using commercially available computer software such as SAP2000. The procedure used to design a PFD is described as follows.

1. Analyze the frame structure controlled with a passive friction damper of various friction forces under several earthquake ground motions scaled into the same peak ground acceleration. Plot the story drift and absolute acceleration of the frame as a function of the friction force for each earthquake record and determine the range of friction force corresponding to the minimum story drift and floor acceleration.
2. Plot the accumulative energy diagrams of the frame structure for each earthquake to ensure the energy dissipation capability of the dampers under consideration, especially in the range of friction force identified in Step 1.
3. Plot the maximum story drift and floor acceleration as a function of the peak ground acceleration and generalize the friction force range selected in Step 1 to take into account the effect of earthquake intensities.
4. Select durable materials as sliding surface and determine the clamping force necessary to provide the required friction force.
5. Design piezoelectric stack actuators (diameter, thickness, and number of layers) to deliver the required clamping force.

3.2 Performance of a PFD under constant voltage supply

When a constant voltage is supplied to the piezoelectric actuators in a PFD, the semi-active friction damper behaves like a passive device. Under this circumstance, the seismic performance of the PFD can be studied with the use of a passive friction damper. The maximum friction force of the damper is held constant during each ground motion application. This process is iterated while changing the friction force.

The 3-story building structure was analyzed using SAP2000 computer software. The frame structure with a passive friction damper was subjected to two far-field earthquake records (the 1940 El Centro and the 1952 Taft earthquakes) and four near-fault records (the 1994 Northridge, the 1995 Kobe, the 1999 Taiwan and Turkey earthquakes). Both far-field and near-field earthquakes are selected in design for later demonstration of the damper’s adaptability to multi-level and multi-type earthquake inputs. All the seismic inputs were scaled to a peak acceleration of 0.26 g (g is the gravitational acceleration). The maximum friction force of the damper ranges from 0 to 10 kips. The maximum story drifts and the maximum absolute accelerations corresponding to different friction forces are presented in Figs. 4 and 5, respectively.

Several observations can be made at the upper and lower friction force limits. As the friction force approaches to zero, the control effects of the passive damper disappear. The story drift and acceleration approach to their respective values present in the uncontrolled structure. On the other

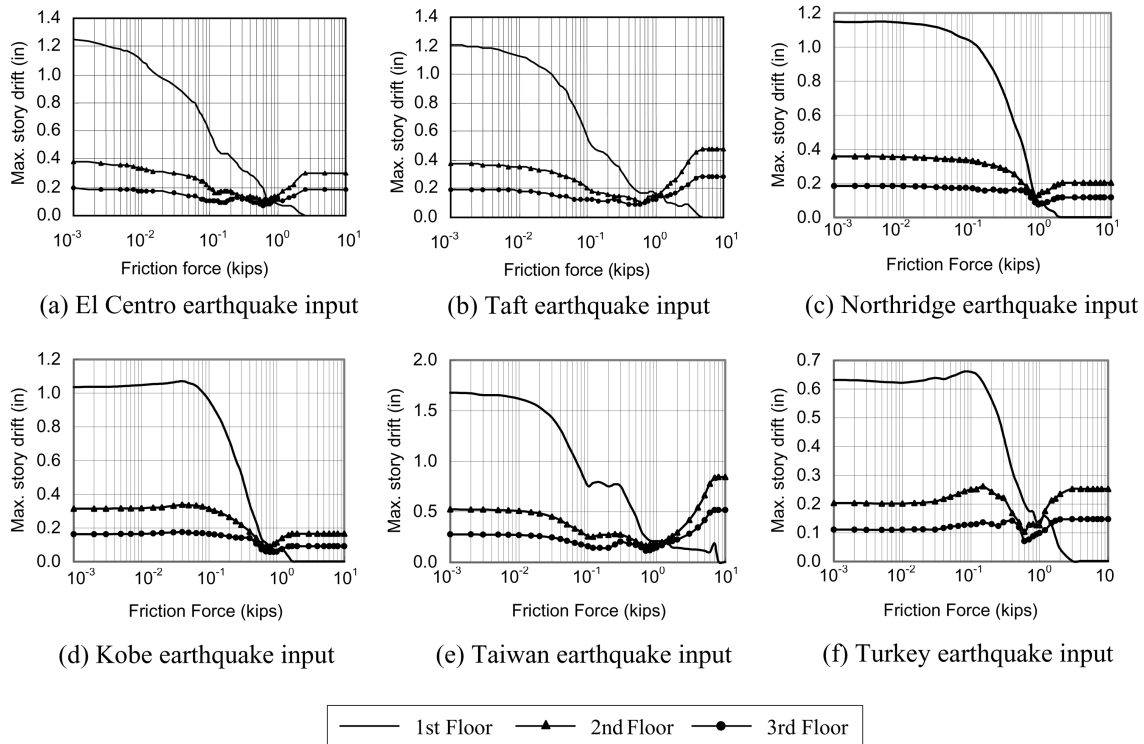


Fig. 4 Peak story drift versus friction force: peak ground acceleration = 0.26 g

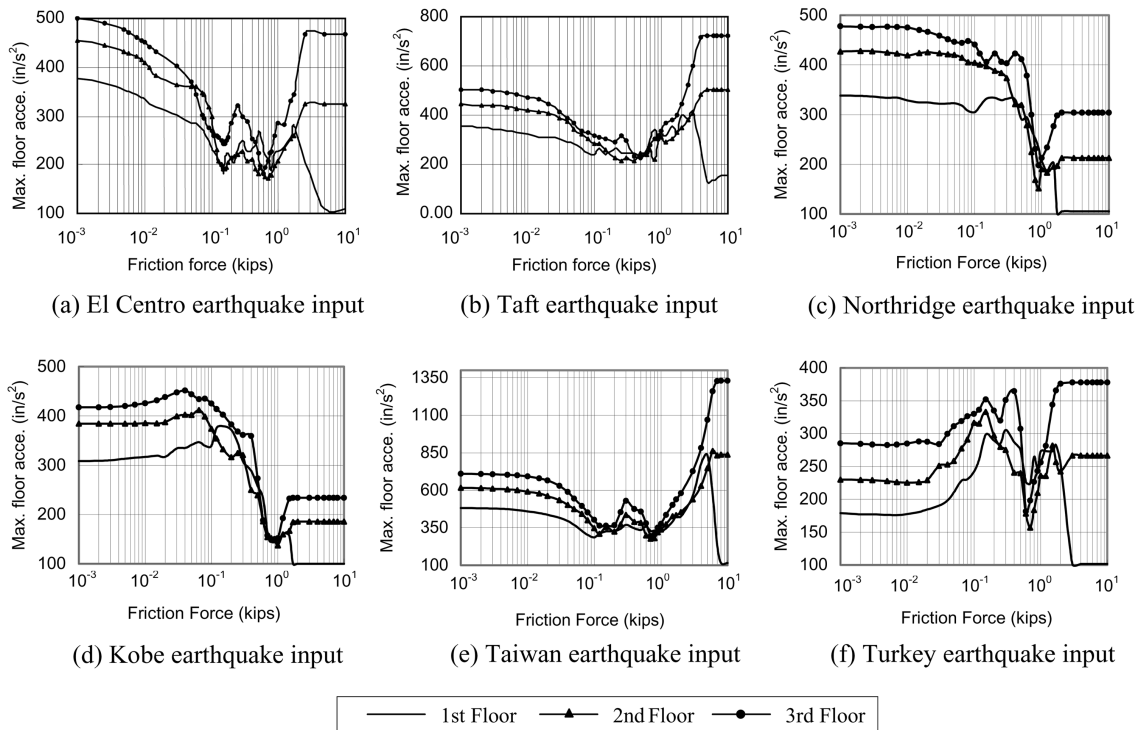


Fig. 5 Peak acceleration versus friction force: peak ground acceleration = 0.26 g

hand, when the friction force becomes very large, the damper does not slide during earthquakes and therefore, both story drift and acceleration are constant. It can be clearly observed from the figures that the drift of the first story always decreases as the friction force increases due to the damper's restraint. Although the various story drifts and accelerations reach their minimum values at different friction forces, all of them are relatively small when the friction force ranges from 0.5 to 0.9 kips, regardless of the near-fault or far-field earthquake effects. Considering the two objectives of minimizing story drift and acceleration, the optimum friction force is taken as 0.75 kips.

To ensure the energy dissipation capability of the friction damper, the accumulative energy diagrams of the structure are shown in Fig. 6 when the structure is subjected to the scaled El Centro and Northridge earthquakes. Three levels of the friction force considered are 0.3, 0.75 and 1.0 kips. As one can see, the energy dissipated by the friction damper and structural damping always increases with time due to accumulation of the dissipation while the mechanical energy (kinetic plus potential) varies over the time. The energy dissipated by the damper constitutes a significant portion of the total input energy. The maximum mechanical energy stored in structure is the largest for 0.3 kips of friction force and the smallest for 0.75 kips. It is also interesting to see that both the energy dissipated by the damper and the total input energy are clearly the largest for the smaller friction force. A damper set to a larger friction force is unlikely in "sliding" state under small motions whereas a damper of a smaller frictional force slides under small motions and therefore dissipates more energy. The former also spreads the mechanical energy over a longer period of time due to friction effects. At a much smaller friction force, the mechanical energy is generated in a short period for the Northridge earthquake reflecting the near-fault characteristics.

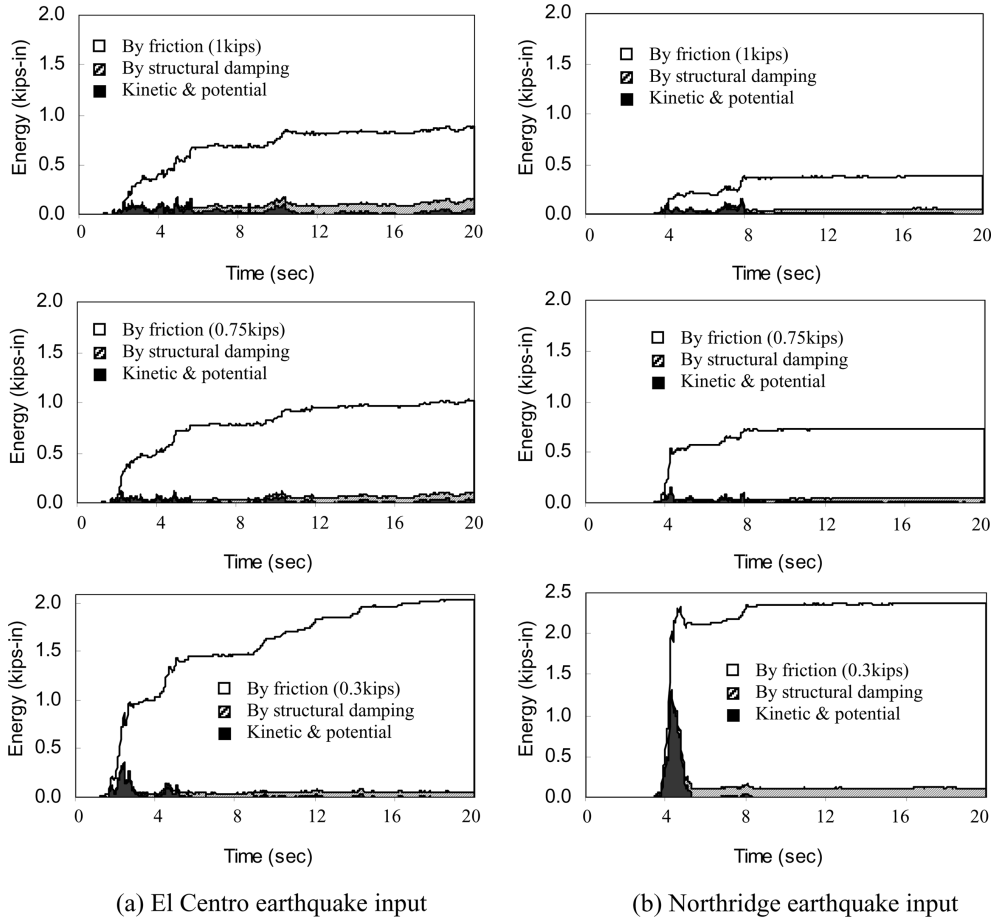


Fig. 6 Accumulative energy diagrams: peak ground acceleration = 0.26 g

The previous analyses were carried out under earthquake-induced ground motions of the same maximum acceleration. A structure, however, may be subjected to earthquakes of various magnitudes during its life span. It can be proven from the equation of motion of the structure that the ratio between the floor acceleration and the peak ground acceleration depends only on the ratio between the friction force and the peak ground acceleration. As seen in Fig. 5, the frame structure often experiences the maximum acceleration at the third floor under various excitations. The maximum acceleration at the third floor is thus plotted as a function of the peak ground acceleration in Fig. 7. Each line in Fig. 7 corresponds to a specified friction force. When the peak ground acceleration ranges from 0.22 g to 0.36 g, the maximum floor acceleration is reduced the most with a 0.75 kip damper. When the peak ground acceleration lies between 0.12 g to 0.22 g, the floor acceleration becomes minimum when the friction force is equal to 0.4 kips. Based on the numerical simulations, the minimum floor acceleration occurs when the friction force of the damper in kip ranges approximately from 2.2 to 3.3 times the peak ground acceleration (g). When the peak ground acceleration is 0.26 g, the friction range is 0.57~0.86 kips.

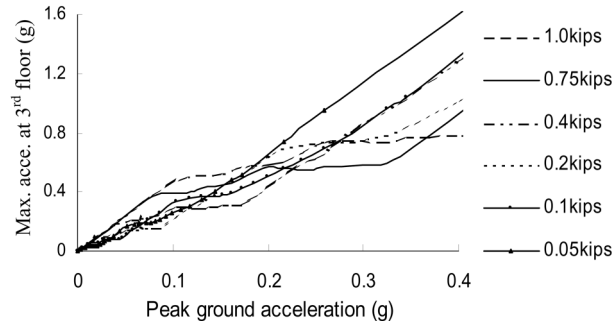


Fig. 7 Peak responses due to excitations of different intensities

3.3 Modulus of elasticity and free displacement of piezoelectric actuators

The two mechanical parameters that directly affect the performance of a piezoelectric stack actuator are the modulus of elasticity and the free displacement when the actuator is free to expand. The effective modulus of elasticity of the actuator assembly can be greatly influenced by the electrode-isolator configuration between adjacent layers. The manufacturer specified the ceramic modulus, but the effective modulus of the amassed actuator was not provided. Therefore, the modulus and free displacement were measured with several laboratory tests. Since the free displacement of an actuator is extremely small, the four actuators in the PFD were stacked in series to magnify the effective free displacement under a given load. The actuators were taped together, placed between two ½-inch-thick flat ground plates, and set between two jaws of a MTS880 loading machine. The displacement was measured by using an extensometer with a two-inch gage length and accuracy of 0.001 in.

The modulus test was performed in the displacement control mode. No electric load was applied to the actuator during testing. The actuators were loaded in one cycle from 340 lbs to 3700 lbs. Each condition was repeated for three times to ensure the quality of test data. Results show an experimental modulus of 4960 ksi, 26% lower than the piezoelectric material modulus of 6700 ksi. The free displacement test was carried out with the MTS machine in its load control mode. The stroke of the unit was set to its minimum. A preload of 340 lbs was applied to the actuators. The voltage was then run through a cycle from 0 to 1000 Volts. The cumulative free displacement of the four actuators was 2.3×10^{-3} in. or approximately 5.8×10^{-4} in. for each stack, which is very close to that given by the manufacturer. In the following, the manufacture-specified free displacement, 6×10^{-4} in., is used.

3.4 Minimum stiffness requirement

A piezoelectric stack actuator can develop a significant stress in its axial direction only when it is tightly clamped or restrained against displacement in that direction. Based on the measured modulus of elasticity, one piezoelectric stack actuator (PZWT100) can theoretically contribute 4.87 kips of clamping force in the fully constrained condition or has a free displacement of approximately 6×10^{-4} inches in the unrestrained or free condition. The fully restrained condition is, however, practically impossible to achieve in applications due to elastic deformation of the system and slack at joints and interfaces. The clamping force of an actuator is inversely proportional to the

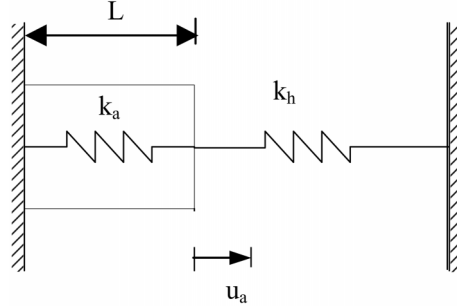


Fig. 8 Two spring model of a PFD

displacement of the mechanical components. Therefore, the flexibility of the mechanical components greatly affects the performance of a PFD.

The PFD being designed includes actuators and other components that are connected in series. The actuators and other components can be simply represented by a model with two springs in series, Fig. 8. The spring with a coefficient $k_a = AY_{33}^E/L$ represents the actuators with their end displacement denoted by u_a . Here A and L are the cross-section area and length of the actuators, respectively. The spring with a coefficient, k_h , called housing stiffness, represents the other mechanical components. As k_h goes to zero, the actuator boundary conditions simulate an unconstrained condition. As k_h becomes infinity, the actuator boundary conditions tend towards a fully constrained condition.

The electric field in Eq. (1) is equal to the voltage (V) divided by the distance between the charged plates or the thickness of a single layer (t). The actuator stress is equal to the force of the actuator, P , over its cross sectional area, A . Consider a compressive load to be positive. Substituting these equalities into Eq. (1) gives the following:

$$\frac{u_a}{L} = -\frac{P}{AY_{33}^E} + \frac{Vd_{33}}{t} \quad (2)$$

where L is the total length or height of the actuator. Since both ends of the spring model in Fig. 8 are fixed, the axial displacement on the actuator is equal in magnitude but opposite in direction to the housing displacement. The actuator displacement can thus be expressed by $u_a = P/k_h$. Substituting this relation into Eq. (2) leads to the expression for the housing stiffness,

$$k_h = \frac{P}{Vd_{33}L/t - P/k_a}. \quad (3)$$

Piezoelectric actuators exhibit hysteresis behaviors as illustrated in Fig. 1. For practical design purposes, however, a quasi-linear approximation between the free displacement (u_a^{free}) and the applied voltage (V) can be made. In this case, the quantity $Vd_{33}L/t$ in Eq. (3) corresponds to the free displacement, u_a^{free} , as derived from Eq. (2) by setting $P = 0$. Therefore, the minimum housing stiffness, $k_{h, \min}$, for the required control force, P , can be determined by

$$k_{h, \min} = \frac{P}{u_a^{free} - P/k_a}. \quad (4)$$

It is noted that the above approximation leads to an equivalent length of the actuator, $L_{eq} = u_a^{free} t / Vd_{33}$. The equivalent length should be used throughout the design of the damper for consistency.

3.5 Size of a PFD

Several factors were considered in the design of the prototype PFD. The damper must include a mechanism by which the initial force on the actuators can be adjusted to minimize slacks among various mechanical components. The damper also had to be designed around existing geometric parameters that occurred on the 1/4-scale, three-story structure for ease of installation (Tian 1997).

Numerical analysis in Section 3.2 indicated that the optimum operation friction range of the prototype PFD is approximately 0.57~0.86 kips. Considering brake linings as friction materials, a friction coefficient of 0.85 can be used in design, which was obtained from the test results in Section 5.2. The operating friction range of 0.57~0.86 kips translates into a range of clamping force of 0.67~1.01 kips. The lower bound of 0.67 kips can be provided with passive mechanisms and the range of 0.34 kips will be generated by piezoelectric actuators with the applied voltage of 1000 Volts. The PFD to be designed includes four preloading units and four piezoelectric stack actuators that are symmetrically arranged in parallel. Using the KCI actuator of 1 inch in diameter with each layer of 0.02 in. thick, the stiffness of the four stack actuators in parallel is $k_a = 4AY_{33}^E/L_{eq} = 18960$ kip/in using the measured modulus of elasticity. The minimum housing stiffness from Eq. (4) is $k_{h, min} = 584$ kip/in. based on the free displacement of 6×10^{-4} in. at 1000 Volts. Note that the number of piezoelectric layers (24 in this case) is determined to correspond to the free displacement used in the design. This information can be obtained from the manufacturer.

For ease of the installation of four stack actuators, a steel box of 10 in. long, 6 in. wide, and 4 in. tall was selected. The steel box shown in Fig. 2 is to be bolted together from several plates. The clamping force on the piezoelectric actuators is reacted by the top plate of the damper. Under the four reaction forces from the actuators, a plate of 1/2-inch thick can provide a stiffness of approximately 650 kip/in at the loading points, which was estimated with a simply-supported beam on the conservative side. The plate stiffness provided exceeds the minimum required stiffness of 584 kip/in. The final design of the PFD is schematically shown in Fig. 2(b).

4. Fabrication of the prototype PFD

During the damper fabrication, special attentions were paid to preventing the isolation plate from moving in any planar direction while still allowing vertical movement and to keep the preloading bolts fixed during the tests. A solution to the first issue was accomplished by employing two bolts with rounded ends located at each orthogonal, inner housing surface. To restrict the isolation plate's in-plane movement, these round-ended bolts are extended until snug against the isolation plate. To keep the preloading bolts and the isolation plate restraining bolts fixed at the desired position, jam nuts were implemented. After the preloading bolts or isolation bolts are adjusted to the desired position, these nuts are tightened to prevent the bolts from vibrating loose.

A major concern during fabrication was the small tolerances imposed on the damper by the behavior and properties of the piezoelectric actuators. Great care was taken to ensure that the housing surfaces were flat and normal to one another and the connections were tight and rigid. The housing was constructed of half-inch cold-rolled flat steel and held together with 1/4 inch diameter bolts. The preloading anchor, load cell cap, and preloading platforms were constructed from 2 inch diameter cold drawn steel rods.

Another task during the fabrication process was the bonding of the friction material to the metal

plate to form the friction plate assembly. Sandwiched between the isolation plate and the bottom plate of the housing, the friction plate consists of a 1/16 in. thick plate 4.25 inches wide with friction material $3/16 \times 4.25 \times 9$ in sections bonded to both sides.

The assembly was bonded together with a 3M Scotch-Weld™ 2216 B/A^{Gray} Epoxy Adhesive. A thin layer of the bonding agent was applied to the friction material. The sections of friction material were then set against the metal plate. A clamping force of approximately 300 lbs was applied during the curing process by using the Tinius Olsen testing machine. The assembly was left in the clamped state for five days. The friction material flatness and the bond surface was inspected and approved. More detailed information on the fabrication process can be found in Garrett (2002). The final product of the fabrication is the prototype PFD presented in Fig. 2(a).

5. Experimental characterization of the prototype PFD

5.1 Test setup and instrumentation

A 22-kip MTS hydraulic actuator was used to apply a harmonic displacement to the damper. It has a dynamic stroke of 6 in. and a static stroke of 6.6 in. An MTS436 Control Unit and MTS406 Controller were used to control the actuator. The MTS436 is a function generator that commands the on-off of the hydraulic power and generates displacement signals of different frequencies and waveforms for the MTS406 controller to control the hydraulic actuator for any required movement. The system is capable of producing 0.01-10 Hz signals.

The test instrumentation consisted of a 2-kip load cell for measuring the horizontal friction force, four 5-kip pancake load cells for measuring the clamping force in each of the four stack assemblies, and an linearly variable differential transformer (LVDT) for measuring the horizontal displacement. The LVDT was attached to the friction plate frame as marked on Fig. 9 together with the testing instrumentation and instrument location.

Two Power Amplifier/Piezo Drivers, Model KC 700 from KCI, power the actuators. They are DC-stable power amplifiers designed to provide precise control of output voltages. The manufacturer altered the range of output voltage from the original 0~700 Volts to 0~1000 Volts. Each unit

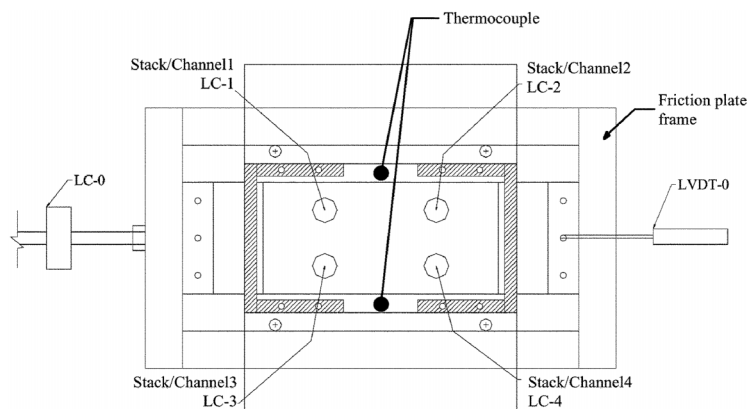


Fig. 9 Instrumentation location

consists of two channels of amplified outputs. An input voltage of 0 to 10 Volts dynamically controls each channel. The amplifier magnifies the input voltage by a gain of 200. The channels are numbered 1 through 4 corresponding to the stack number it drives in the damper as indicated in Fig. 9. A VXI data acquisition and control workstation was used to control the output voltage of each channel. A new control program was written to linearly increase and decrease the input voltages with respect to time from 0 to a predetermined value.

5.2 The prototype PFD in a passive state

It is imperative that the characteristics of the damper under a passive state be well understood before semi-active operations were studied. Therefore, all tests in this section were performed with no applied voltage. Before each test, the hydraulic actuator was set to its equilibrium position and the preloading bolts were set to the desired clamping force.

Tests were performed for a twenty-second duration at preloads of 160, 240, 400, and 800 lbs and at a displacement of approximately ± 0.25 in. At each preload, the damper was tested at ten frequencies of 0.4, 0.8, 1.1, 1.4, 1.8, 2.0, 2.7, 3.4, 4.9, and 5.9 Hz. The data generated during each testing sequence were analyzed to determine the coefficient of friction of the damper and its energy dissipation per cycle.

From the extensive test data (Garrett 2002), it can be observed that the force-displacement loops of the damper are nearly independent of the frequency and proportional to the clamping force present in the damper. The typical force-displacement loops are shown in Fig. 10(a). They are stable and all nearly rectangular in shape. A small non-uniformity appears in the hysteretic loops as the friction force slightly increases from the maximum displacement to the minimum displacement. This insignificant increase may result from uneven friction surfaces though every effort was made during fabrication to make it as flat as practically could. Consistent with the hysteresis loop irregularity, the clamping force oscillates at the excitation frequency as indicated in Fig. 10(b). The mean clamping force increases and gradually stabilizes with respect to time. The increase may not be a concern for higher preloads during a short period of earthquake disturbance. When the damper stops, the incremental clamping force gained during the operation period disappears. For the same reason, the damper experiences a larger positive displacement.

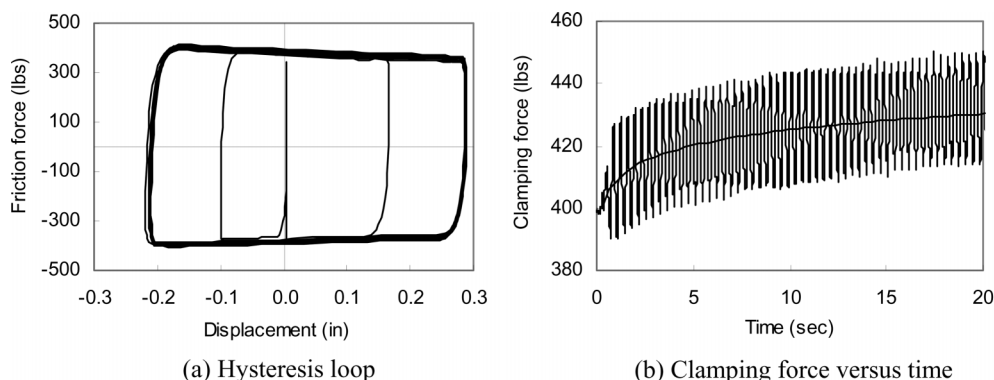


Fig. 10 Damper behavior in passive state: 400 lbs preload and 2.8 Hz. frequency

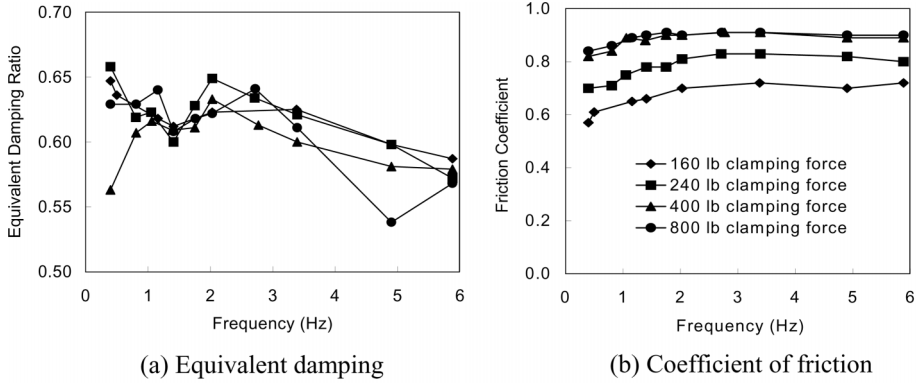


Fig. 11 Characterization test results graphed as a function of frequency

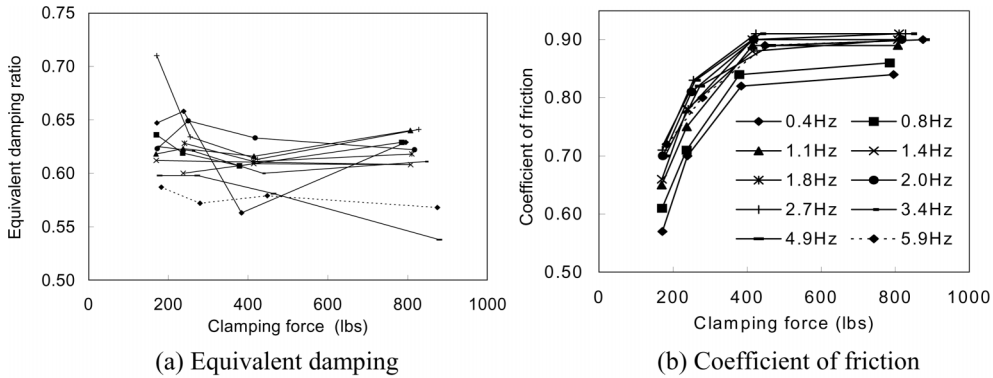


Fig. 12 Characterization test results graphed as a function of clamping force

The coefficient of friction and equivalent damping ratio were studied as a function of frequency, shown in Fig. 11, and clamping force in Fig. 12. The equivalent damping ratio is defined in a way similar to the equivalent viscous damping in structural dynamics except that the restoring energy is replaced with half of the maximum friction force times the maximum displacement. The equivalent damping ratio seems fairly independent of frequency and clamping force as shown in Figs. 11(a) and 12(a). The test values lie between 0.55 and 0.65 with an average of 0.61. It decreases slightly with increasing frequency from approximately 0.65 at a frequency of 0.4 Hz. to 0.57 at 5.9 Hz. The coefficient of friction increases slightly with increasing frequency up to 2 Hz, Fig. 11(b), but increases significantly with clamping force as indicated in Fig. 12(b). From 400 to 800 lbs of clamping force, however, the coefficient of friction is practically constant. An average value of 0.85 has been used in design of the PFD.

5.3 The prototype PFD in a semi-active state

When both voltage and preload are applied on the PFD, it is considered in a semi-active state. A series of tests were performed to study the piezoelectric actuator's capabilities in meeting the design objectives. This was accomplished through the application of voltages to the actuators with no horizontal excitation present in the system or in the static state. When each actuator is subjected to a

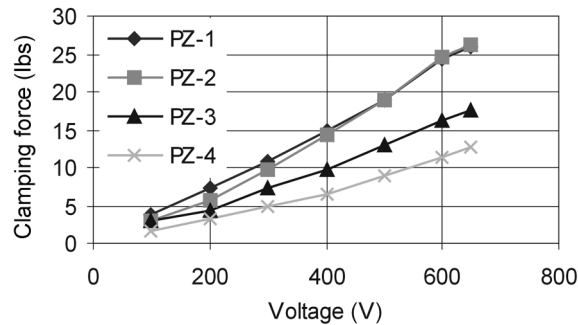


Fig. 13 Incremental clamping force due to applied voltage: 20 lbs preload

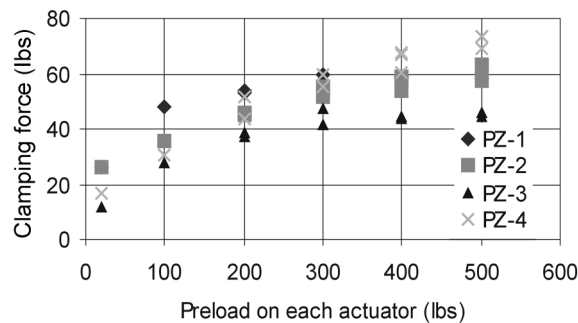


Fig. 14 Incremental clamping force versus preload: 650 V voltage

preload of 20 lbs, the clamping force generated in a stack actuator by applying various voltages is plotted in Fig. 13. The clamping force increases with the applied voltage in a nearly linear fashion, reflecting the weak hysteresis behavior of the actuators in the range of the applied voltage. It can also be seen from the figure that the clamping forces of the four actuators deviate more as they are subjected to a higher voltage.

To understand how preload affects the behavior of actuators, a series of tests at 650 Volts applied on each actuator simultaneously were conducted with different preloads. Fig. 14 presents the clamping force in each stack actuator generated by the applied voltage. Three trial runs were carried out for each condition to validate the test data. It can be seen that the clamping force increases rapidly with preload and slows down as the preload continues to increase. These results agree with the general conclusions on piezoelectric stack actuators drawn by Mitrovic *et al.* (2000).

The performance of the actuators can now be evaluated against the original design. It is recalled that the original design used a total preload of 0.67 kips on four actuators as discussed in Section 3.5; each carried approximately 0.17 kips. At this level of preload, each actuator is capable of generating a clamping force of approximately 34 to 53 lbs as interpolated from Fig. 14. This incremental clamping force translates into a damper friction force range of 0.12 to 0.18 kips at 650 Volts. Considering a linear relation between the clamping force and the applied voltage as indicated in Fig. 13, the total friction force was extrapolated into 0.18~0.28 kips at 1000 Volts, which corresponds to 62~97% of the design value ($0.85 \times 0.34 = 0.29$ kips, Section 3.5). The average friction force that the damper can generate at 1000 Volts is 0.23 kips, which is 21% less than the design value. The low loading capability reflects the variation of the actuator's behavior and the accumulative flexibility from all mechanical components in the PFD.

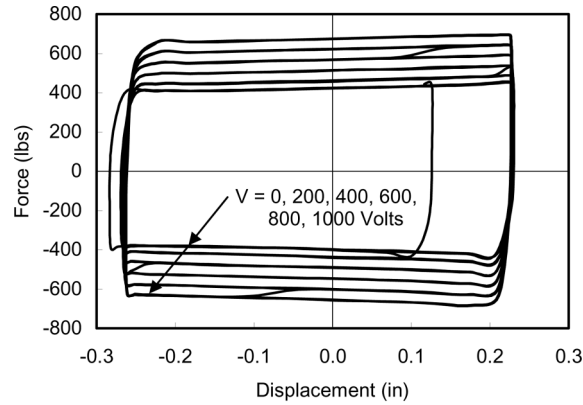


Fig. 15 Hysteresis loop at various voltages

To verify the actuators' behavior with horizontal motions, the prototype damper was again tested under harmonic loading with the four 5-kip load cells removed. At a preload of approximately 470 lbs on the damper, the force-displacement hysteresis loops of the damper is shown in Fig. 15 for an applied voltage of 0, 200, 400, 600, 800, and 1000 Volts. It can be determined from the figure that the friction force range is about 0.26 kips, which is approximately 90% of the design value of 0.29 kips at 1000 Volts. Under a higher preload, the load generating capability will increase as inferred from Fig. 14. It is noted that this test was conducted on the damper after being rotated for 180° in plan. In this case, the damper moves more toward the negative displacement in comparison with Fig. 10(a). The purpose of rotating the damper was to confirm the effect of a slightly uneven friction surface on the non-uniformity in load-displacement relation.

5.4 Durability testing

During its service life, a damper can experience many cycles of loading. Its temperature change over the time is a concern in engineering applications. Two thermal couplers were deployed on the damper as shown in Fig. 9. These temperature-sensing devices were positioned on opposite sides of the damper's bottom plate close to the bottom friction surface. The couplers ran to an independent thermal-coupler box. The tests were run for 12,000 cycles at a 400-pound preload. The test was run three times at different frequencies of 1, 3, and 5 Hz. The temperature data were recorded manually at the test start and every 2000 cycles after.

Table 1 Measured temperature in °F on the PFD

Cycles (×2000)	Temperature at Near Side			Temperature at Far Side		
	1 Hz	3 Hz	5 Hz	1 Hz	3 Hz	5 Hz
0	62	77	66	62	74	66
1	76	100	96	76	94	96
2	84	110	95	82	105	94
3	86	115	97	85	110	97
4	85	121	99	84	115	101
5	87	113	100	85	109	101

The temperatures measured during the durability tests are presented in Table 1. It can be observed from the table that the friction surface temperature initially increases at a high rate, but levels off considerably after the first 2000 cycles. The temperatures at the near and far side are generally close, indicating a relatively even distribution of the clamping force on the friction plate across the damper's movement. Overall the friction surface heat production is not significant enough to be a detriment to the friction material and bonding interface.

6. Conclusions

A practical procedure has been proposed to size a PFD using commercial computer software for peak response reduction of the 1/4-scale three-story steel frame structure. A prototype friction damper has been designed, fabricated, and tested to characterize its dynamic properties in the laboratory. Based on the numerical and experimental simulations, the following conclusions can be drawn:

1. To effectively reduce both the story drift and floor acceleration of the 1/4-scale frame structure, an operation friction force (kips) between 2.2 and 3.3 times the peak ground acceleration (g) is required under earthquake loads, regardless of near-fault or far-field earthquakes. When the peak ground acceleration is equal to 0.26 g, the optimum value of the maximum friction force is estimated to be 0.75 kips.
2. A 10" × 6" × 4" friction damper has been designed and fabricated in the laboratory. It consists of four loading units to remove any slack in the load path, four piezoelectric stack actuators to regulate the clamping force on the damper, a frictional surface sliding plate, and a steel box to house other components. Each stack actuator has 24 discs of PZWT100 materials and each disc is 0.020 in. thick. The actuator's modulus of elasticity is 26% lower than that specified by the manufacturer.
3. The performance of the prototype friction damper was proven consistent with a number of characterization tests. The force-displacement loops under harmonic loading were nearly rectangular in shape and independent of the excitation frequency. The coefficient of friction of the brake linings is approximately 0.85 when the clamping force on the damper is above 400 lbs. The equivalent damping was found to slightly decrease with the frequency and the clamping force, with an average value of 0.61.
4. The durability of the prototype damper is not a concern. The temperature in the proximity of the friction materials rises at the beginning of the test and rapidly approaches a constant. Although the clamping force fluctuates around an average value increasing with time, the change in clamping force is insignificant during a short operating period.
5. Based on the characterization test results, a preload of 170 lbs/actuator and the range of clamping force of 50~80 lbs/actuator are determined to satisfactorily reduce the story drifts and accelerations of the 3-story building frame.
6. The adaptability of the damper with the applied voltages of 0~1000 Volts was found to be approximately 90% of the expected. The low friction force range reflects the variation of the actuators' behavior and the accumulative flexibility of all mechanical components in the PFD.

To increase the loading capability of the prototype damper, future researches will be directed into the following three areas. First, the next generation PFD will be designed and fabricated with multiple friction plates so that the friction force is proportionally increased. Secondly, to compensate for the friction force loss due to the flexibility in mechanical components, the minimum stiffness of

the top plate will be selected corresponding to a higher force P in Eq. (4), say twice or more. Lastly, to further reduce the flexibility of mechanical components in series with the piezoelectric actuators, the friction pads on two sides of a friction plate will be made thinner.

Acknowledgements

This study was sponsored in part by the U.S. National Science Foundation under Award No. CMS9733123 with Drs. S.C. Liu and P. Chang as Program Directors and by the Intelligent Systems Center at the University of Missouri-Rolla. These supports are gratefully appreciated. The results, opinions and conclusions expressed in this paper are solely those of the authors and do not necessarily represent those of the sponsor.

References

- Akbay, Z. and Aktan, H.M. (1990), "Intelligent energy dissipation devices", *Proc. 4th U.S. National Conf. Earthquake Engrg.*, May 20-24, Palm Springs, CA, 427-435.
- Chen, Genda and Chen, Chaoqiang. (2000), "Behavior of piezoelectric friction dampers under dynamic loading", *Proc. SPIE's 7th Int. Symp. on Smart Struct. and Mater.*, March 5-9, Newport Beach, CA.
- Chen, Genda and Chen, Chaoqiang. (2002a), "Control of plastic deformation of steel moment-resisting frame structures with active friction dampers", *Proc. 7th U.S. National Conf. Earthquake Engrg.*, July 21-25, Boston, MA.
- Chen, Chaoqiang and Chen, Genda. (2002b), "Nonlinear control of a 20-story steel building with active piezoelectric friction dampers", *Int. J. Struct. Engrg. Mech.*, **14**(1), 21-38.
- Chen, Genda and Chen, Chaoqiang. (2002c), "Building hazard mitigation with piezoelectric friction dampers", *Proc. Int. Conf. Adv. Bldg. Tech.*, Dec. 4-6, Hong Kong.
- Dowdell, D.J. and Cherry, S. (1994), "Semi-active friction dampers for seismic response control of structures", *Proc. 5th U.S. National Conf. Earthquake Engrg.*, July 10-14, Chicago, IL.
- Garrett, G.T. (2002), "Experimental characterization of a piezoelectric friction damper", M.S. Thesis, University of Missouri-Rolla.
- Hirai, J., Naruse, M. and Abiru, H. (1996), "Structural control with variable friction damper for seismic response", *Proc. 11th World Conf. Earthq. Engrg.*, June 23-28, Acapulco, Mexico.
- Housner, G.W. *et al.* (1997), "Structural control: past, present, and future", *J. Engrg. Mech.*, ASCE, **123**(9), 897-971.
- Inaudi, J.A. (1997), "Modulated homogeneous friction: a semi-active damping strategy", *Earthq. Engrg. Struct. Dyn.* **26**, 361-376.
- Kannan, S., Uras, H.M. and Aktan, H.M. (1995), "Active control of building seismic response by energy dissipation", *Earthq. Engrg. Struct. Dyn.*, **24**, 747-759.
- Meltzler, A.H. *et al.* (1988), *IEEE Standard on Piezoelectricity*, ANSI/IEEE Std 176 1987, Institute of Electrical and Electronics Engineers, NY.
- Mitrovic, M., Carman, G.P. and Straub, F.K. (2000), "Electro-mechanical characterization of piezoelectric stack actuators", *Proc. SPIE's 7th Int. Symp. on Smart Struct. and Mater.*, March 5-9, Newport Beach, CA.
- O'Neil, C. (2000), "Selected piezoelectric materials and their properties", *Kinetic Ceramics, Inc.*, Personal Communication.
- Soong, T.T. and Dargush, G.F. (1997), *Passive Energy Dissipation Systems in Structural Engineering*, John Wiley & Sons, UK.
- Tian, P. (1997), "Generalized optimal control of elastic and inelastic structures subjected to earthquake excitation", Doctoral Dissertation, University of Missouri-Rolla.